Progress of Theoretical Physics, Vol. 72, No. 2, August 1984

Oscillation and Doubling of Torus

Kunihiko KANEKO

Department of Physics, University of Tokyo, Tokyo 113

(Received February 20, 1984)

Two features of the instability of torus along the amplitude direction are investigated, using various two-dimensional mappings. First, the oscillation of a torus in a delayed logistic map is studied, which is related with the oscillation of an unstable manifold of a periodic saddle. The oscillation is also analyzed from another point of view, i.e., the synergetic effect of the rotation, stretching and folding, which is typically seen in the delayed piecewise-linear mapping. Critical phenomena after the onset of chaos are also discussed. Second, the doubling of a torus is reinvestigated. A torus doubling occurs only a finite number of times. The mechanism of the interruption of the doubling is discussed from three points of view, i.e., relevant perturbation in the RG framework, fractalization and the intermittent-like bursts between the valleys of the multi-humped mapping.

§ 1. Introduction

The onset of chaos from a torus motion is an important problem which has been intensively and extensively studied quite recently.[1)~31)] The instability due to the phase motion of a torus has been investigated by the use of a one-dimensional circle map.[2)~11)] In general problems of the transition from torus to chaos, however, the instability along the amplitude direction is also important, which exhibits novel and interesting features in nonlinear physics. In the present paper we study two problems of the instability of a torus along the amplitude direction by resorting to various kinds of two-dimensional mappings.

An important feature of the amplitude behavior of a torus is the oscillation, which has been observed in a large class of two-dimensional mappings. In experiments on the Bénard convection, the oscillation of a torus was observed by Bergé[23)] and Sano.[29)] In §2, we investigate the two-point delayed logistic map, which shows typically the oscillation of torus (and sometimes of chaos). The oscillation of a torus is understood in connection with the damped oscillation of an unstable manifold of a periodic saddle. Since the unstable manifold is along the amplitude direction, the oscillation of a torus can be regarded as the representation of the instability along the amplitude direction. The experiment by Bergé seems to be well explained by the results in §2.

In §3, we consider the oscillation from another point of view, i.e., a synergetic effect of the rotation, stretching and folding. In order to elucidate this effect we introduce a delayed piecewise-linear mapping, which is a simplified version of the map in §2.

In usual two-dimensional mappings (and the flow with three variables), however, the oscillation is masked by a locking, from which chaos appears via period-doubling bifurcations. In three-dimensional mappings, the doubling of a torus itself is also possible, which has been found by Arnéodo et al.,[13)] Franceschini (for a flow system),[14)] and by the author.[15)] In these examples the doubling occurs only a finite number of times before chaos appears as is shown in Ref.15). In §4, we consider the mechanism of the interruption of the doubling cascade of tori using a coupled circle and logistic map. Its mechanism is understood from three points of view, i.e., first, from a renormalization group viewpoint, and second, from the fractalization of torus,[19)] and lastly by the intermittent-

like burst between the valleys of a one-dimensional mapping with multiple humps.

Section 5 is devoted to discussions.

§ 2. Oscillation of torus

In various two-dimensional mappings, the oscillation of torus appears before the transition from torus to chaos undergoes. In the present section, we give numerical results for a typical mapping and discuss the mechanism of the oscillation. The map we investigate here is the following two-point delayed logistic map,[18]

$$\begin{cases} x_{n+1}=Ax_n+(1-A)(1-Dy_n^2), \\ y_{n+1}=x_n . \end{cases} \tag{2·1}$$

The fixed point of the map $x=y=(\sqrt{1+4D}-1)/(2D)$ loses its stability at $D=1/(1-A)$ via a Hopf bifurcation and a torus appears for $D>1/(1-A)$. As D is increased further, the transition to chaos occurs accompanied by various frequency lockings.[5),12)]

The attractors are given in Figs. 1(a)~(g). Thus, the transition proceeds as follows.

The oscillation of torus (Figs. 1 (a), (b))→various kinds of lockings (Fig. 1 (c))→chaos emerges via a locking (Fig. 1 (d))→the width of "belt-like" attractor along the amplitude direction increases (the dimension becomes two) (Figs. 1 (e), (f))→the unstable fixed point $x=y=(\sqrt{1+4D}-1)/(2D)$ becomes a snap-back repeller[32)](Fig. 1 (g)).

Next, we study the oscillation of torus in more detail. For simplicity, we consider the map (2·1) for smaller values of A, where the locking into a 4-cycle is dominant near the region of the transition to chaos. The oscillation of torus is typically seen near this locking (see Fig. 2). The magnified figures of the attractors are given in Figs. 3(a) (torus), 3(b) (locking) and 3(c) (chaos).

The mechanism of this oscillation is understood as follows: We consider a locking (4-cycle) which appears at a different but close value of the bifurcation parameter. When the locking occurs, periodic saddles (with period-4) also appear. If the unstable manifold

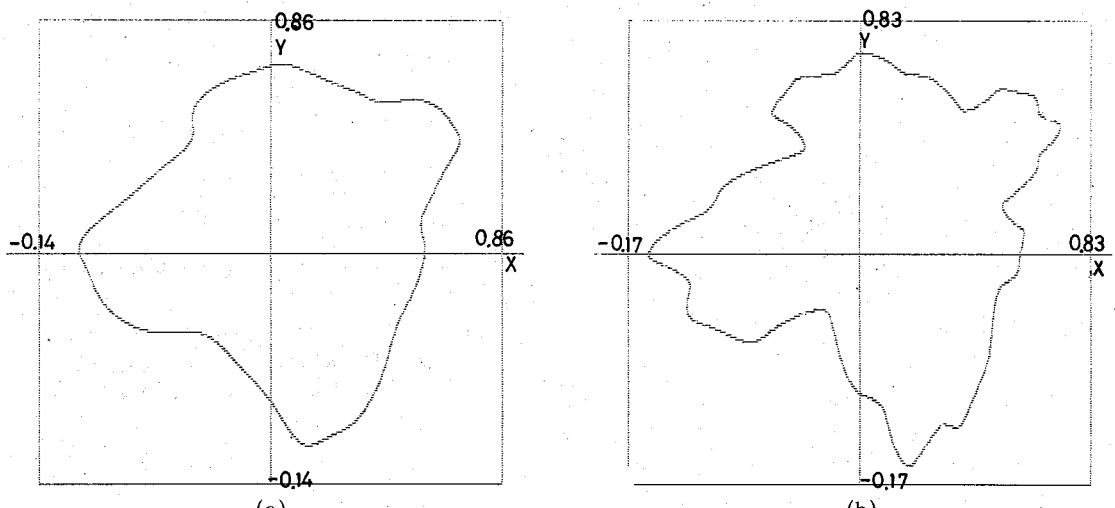

(a) (b)

Fig. 1. (continued)

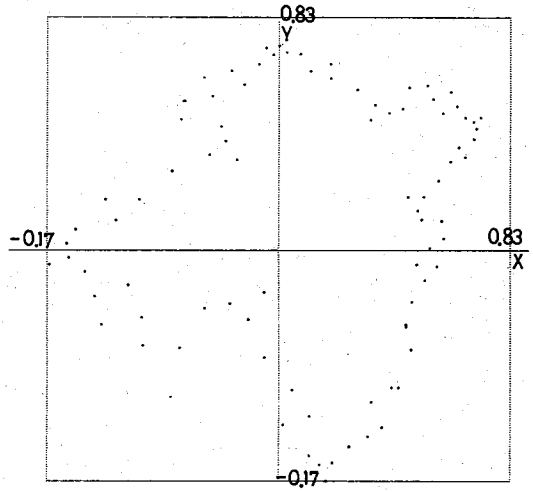

(c)

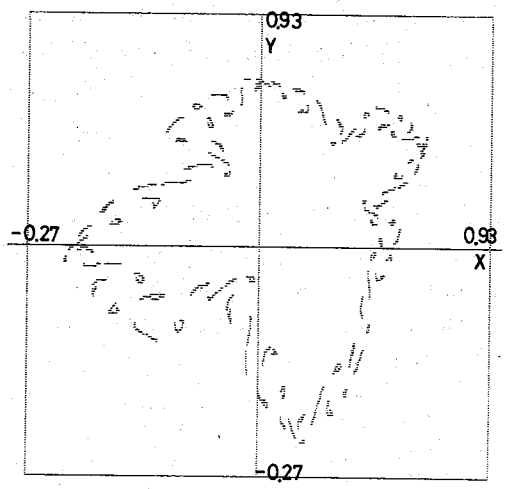

(d)

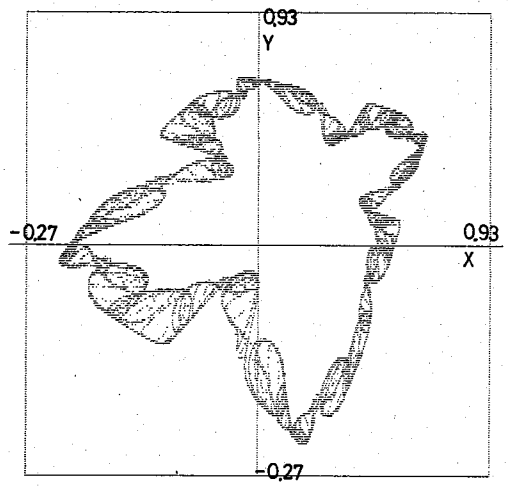

(e)

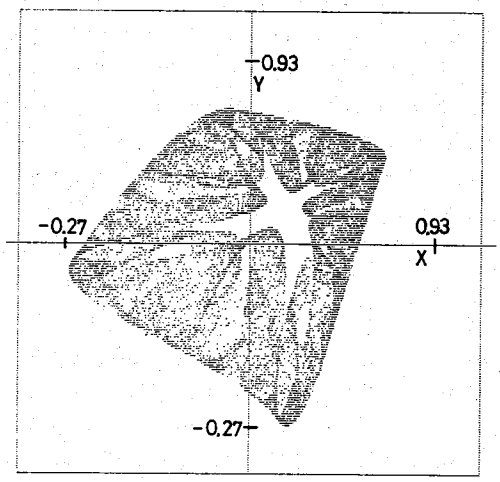

(f)

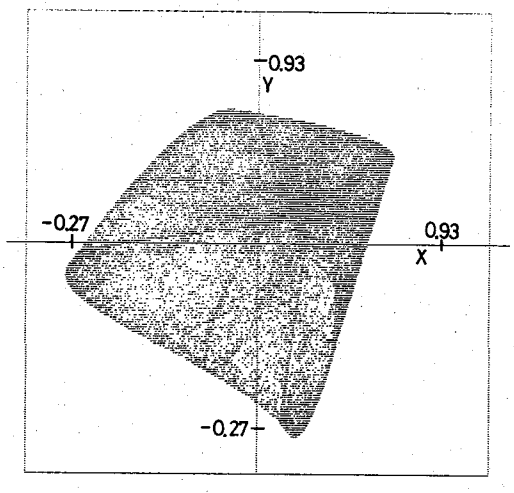

(g)

Fig. 1. Attractor of the delayed logistic map (2·1), with $A=0.3$.
(a) $D=1.75$(torus) (b) $D=1.86$(torus)
(c) $D=1.90$(locking) (d) $D=1.94$(chaos)
(e) $D=1.95$(chaos) (f) $D=2.09$(chaos)
(g) $D=2.16$(chaos)

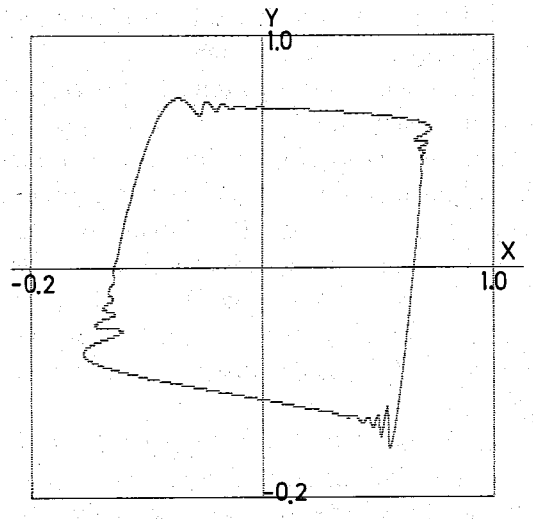

Fig. 2. Attractor of the map (2·1) with $A=0.12$ and $D=1.3$.

of a periodic saddle crosses to a stable manifold of a stable cycle, it must cross infinite times. We investigate the Jacobi matrix $J(x_j^{s(u)}, y_j^{s(u)})$ where $(x_j^{s(u)}, y_j^{s(u)})$ $(j=1, 2, 3, 4)$ are stable (unstable) periodic points. The matrix $J(x_1^s, y_1^s)J(x_2^s, y_2^s)J(x_3^s, y_3^s)J(x_4^s, y_4^s)$ has the eigenvalues λ_{sp} $(0<\lambda_{sp}<1)$ and λ_{sa} $(-1<\lambda_{sa}<0)$, while the matrix $J(x_1^u, y_1^u)J(x_2^u, y_2^u)J(x_3^u, y_s^u)J(x_4^u, y_4^u)$ has the eigenvalues λ_{up} $(\lambda_{up}>1)$ and λ_{ua} $(-1<\lambda_{ua}<0)$ ("p" and "a" represent the "phase" and "amplitude" respectively, while "s" and "u" denote "stable" and "unstable").*) The manifolds corresponding to these eigenvalues are schematically shown in Fig. 4. If the manifolds M_{up} and M_{sp} intersect transversally at P, they intersect also at the points $T^4(P)$, $T^8(P)$, $\cdots$, (T represents the operation of the mapping (2·1)). Thus, the damped oscillation of the unstable manifold appears, which reflects the fact that λ_{sa} is negative. The oscillation is rather analogous to the heteroclinic oscillation in area-preserving mappings, though the oscillation in our case is a damped one. The unstable manifold of a periodic saddle is given in Fig. 5, which was obtained numerically.

When the bifurcation parameter is a little less than A_4 (A_4 is the value of A at which the stable 4-cycle appears), the orbit points stay a long time near x_1^*, x_2^*, x_3^*, x_4^*, where $(x_i^*)(i=1, \cdots, 4)$ are the periodic points at $A=A_4$. Since the motion $T^4(x, y)$ changes continuously against the change of the bifurcation parameter A, the oscillation of the unstable manifold at $A>A_4$ remains as an oscillation of the attractor for $A<A_4$. Thus,

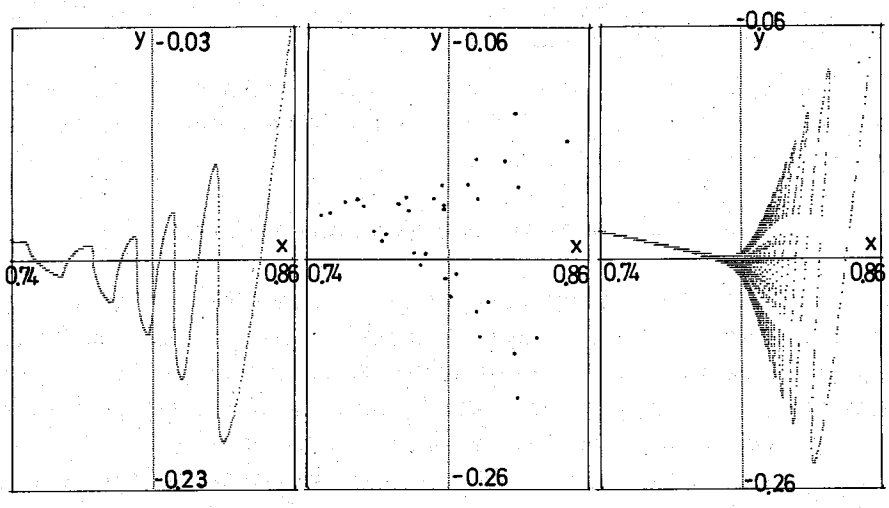

Fig. 3. A part of the attractor of the map (2·1) with $A=0.12$.

*) The two directions correspond to the eigenvectors of the Jacobi matrix. When the torus exists, λ_{sp} goes to 1 (phase direction), while λ_{sa} remains the value between -1 and 0 (amplitude direction).

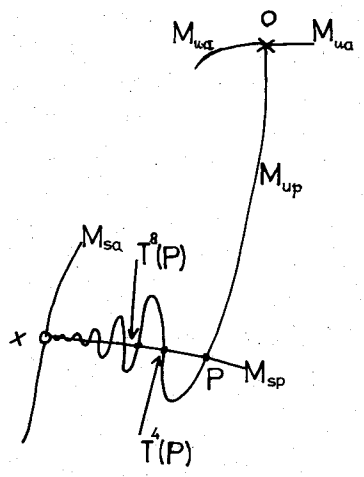

Fig. 4. Schematic representation of stable and unstable manifolds. ○ denotes a stable cycle, while × denotes a periodic saddle. See the text for other notations.

the oscillation of torus is explained from the viewpoint of an unstable manifold.

Since the oscillation damps by the factor λ_{sa}, it is remarkably seen if λ_{sa} is close to -1. In this sense, the oscillatory behavior reflects the instability about the amplitude direction. In our map, the 4-cycle period-doubles along the amplitude direction as A is increased. Thus, the value λ_{sa} is close to -1 at $A<A_4$, which is the reason why the oscillation of torus is clearly seen in our map.

So far, we have illustrated the mechanism of the oscillation of the attractor using the case where the locking to a 4-cycle is dominant. The mechanism, however, is the same even if a locking to a p-cycle is

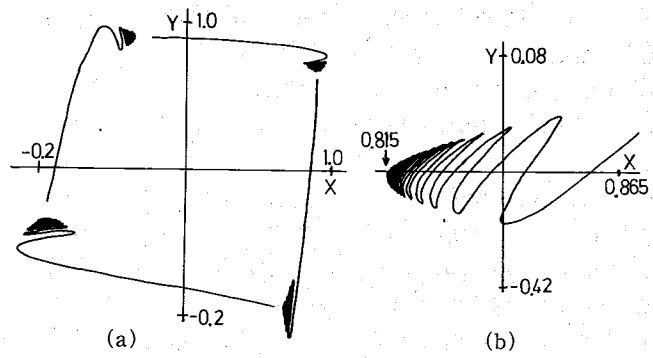

Fig. 5. Unstable manifolds of periodic saddles for the map (2·1) with $A=0.12$ and $D=1.37$, which are obtained numerically. (b) is the enlargement of (a).

dominant. The experiment by Bergé,[23] for example, corresponds to the case where the locking to a 3-cycle is dominant. The oscillation of torus in his experiment seems to be well explained by the above consideration.

§ 3. Rotation, stretching and solding

In the present section we consider the oscillation of an attractor (torus or chaos) from another point of view. We note an unstable focus ($x=y=1/(1+D)$ for the map (2·1)), from which an orbit spirals out. The stretching of an orbit stops if the orbit enters the region $y<0$, where the folding occurs. By the iteration of the mapping, the folding is rotated and stretched, which causes the oscillation of the attractor.

To see the above picture of the oscillation clearly, we simplify the map (2·1) and introduce the following delayed piecewise-linear map,

$$\begin{cases} x_{n+1}=Ax_n+(1-A)(1-D|y_n|), \\ y_{n+1}=x_n. \end{cases} \tag{3·1}$$

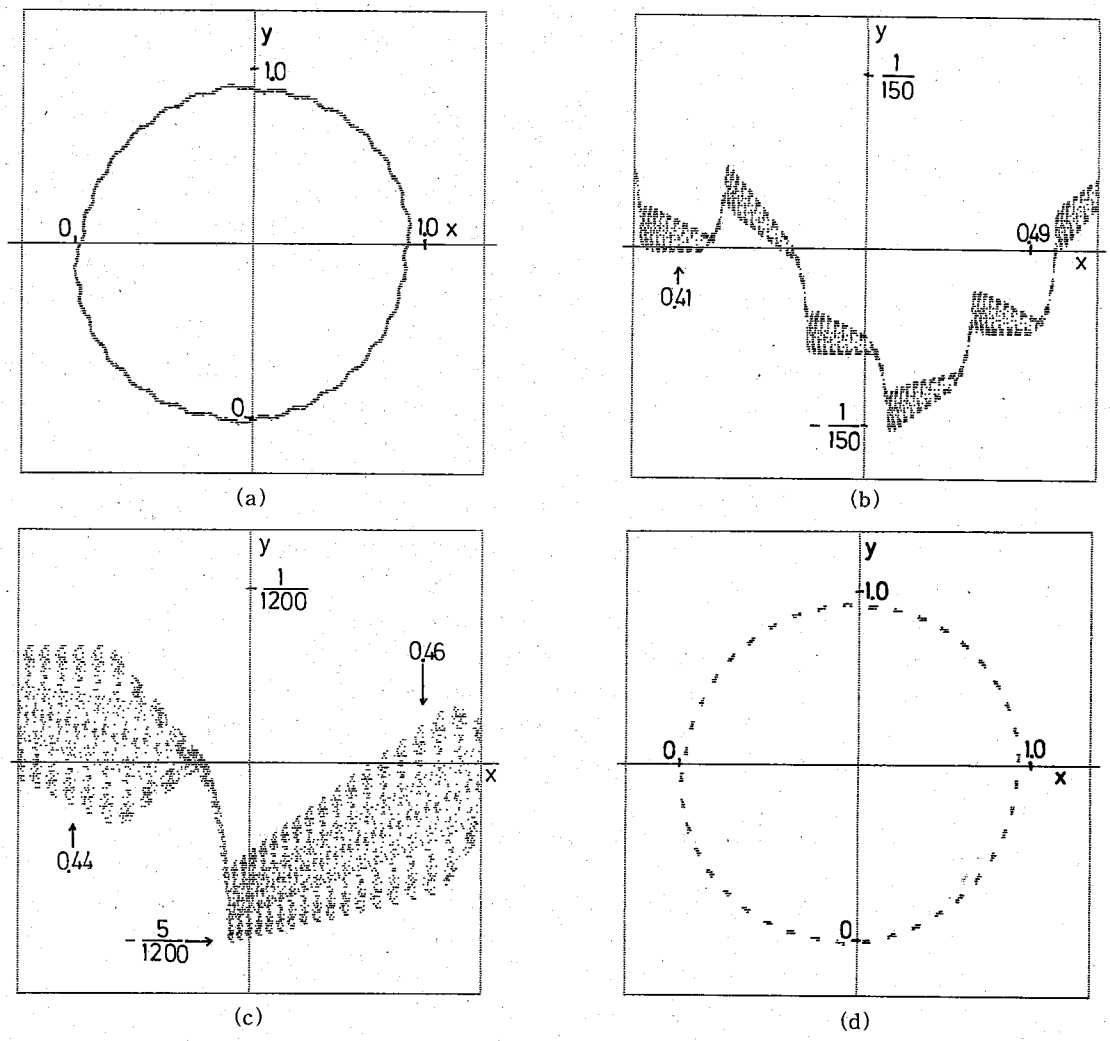

Fig. 6. Attractor of the delayed piecewise-linear map (2·1). The value A is 0.1 for (a)~(c), where the onset of chaos occurs at $D=1/(1-A)=10/9$. (a) $D=1.113$ (b) $D=1.1118$ (only a part) (c) $D=1.1115$ (only a part) (d) $D=1.0834\cdots$, and $A=0.0766\cdots$, The values correspond to $c=1.0008$ and $\vartheta=10/41$. The attractors are splitted into 41 regions.

The fixed point $(x, y)=(1/(1+D), 1/(1+D))$ becomes an unstable focus for $D>1/(1-A)=D_c$. In the map (3·1), chaos appears immediately for $D>1/(1-A)$, which is typical in piecewise-linear mappings. For $y>0$, the map is reduced to a linear transformation (i.e., rotation and stretching)

$$\begin{pmatrix} x'_{n+1} \\ y'_{n+1} \end{pmatrix} = \begin{pmatrix} A & -(1-A)D \\ 1 & 0 \end{pmatrix} \begin{pmatrix} x_n' \\ y_n' \end{pmatrix}, \tag{3·2}$$

where $x'=x-1/(1+D)$ and $y'=y-1/(1+D)$. For $y<0$, the folding occurs by the term $D|y|$.*) The attractors of the map (3·1) are shown in Fig. 6. The oscillatory behavior of

*) It means the transformation $y\to -y$. In the region $y<0$, the direction of the rotation is nearly parallel to the x-axis. Thus, the folding occurs nearly parallel to the amplitude direction in §2.

the attractor is clearly seen, which can be explained by the above mechanism, i.e., rotation (the eigenvalues of the matrix (3·2) are complex), stretching (the absolute values of them are larger than 1) and folding.

The Jacobi matrix for the map (3·1) has the eigenvalues $(A\pm\sqrt{4c-A^2}\,i)$ for $y>0$ and $(A\pm\sqrt{4c+A^2})$ for $y<0$, where c is given by $(1-A)D$. Since the measure for $y<0$ is small near the onset of chaos, we can neglect the contribution from the points $y<0$ to the lowest approximation. Then the Lyapunov exponents are given by $(1/2)\log c$ (first and second exponents are degenerate), which agree with the numerical results within 10^{-3}. Within the above approximation the rotation number ϑ is given by $(1/2\pi)\arccos(A/(2\sqrt{c}))$.

Thus, the Lyapunov exponents behave as L_1, $L_2\propto\varepsilon$ near the onset of chaos, where ε denotes $D-D_c$. The measure of the points for $y<0$, which corresponds to the disordering ratio in the circle map,[11] is estimated by a self-consistent argument,[40] which gives disordering ratio$\propto\varepsilon^{1/3}$, near the onset of chaos.

The oscillation near the onset of chaos $(D>1/(1-A))$ shows a small scale structure as is seen in Fig. 6 and it will be possible and interesting to study the critical behaviors of the oscillations near the onset of chaos, using, for example, the continued fraction expansion method for a given irrational rotation number.

When the rotation number is close to a simple rational value, a phenomenon similar to the band splitting in a logistic map is also possible, as is illustrated in Fig. 6(d), where the rotation number is close to 10/41. The linear map (3·1) has abundant new features of chaos and oscillations which have to be illuminated in future.[40]

§ 4. Mechanisms of the interruption of doubling cascades of tori

Recently doubling cascades of tori as the mechanism of the onset of chaos have been found in a lot of systems, such as 3- or 4-dimensional mappings[13),15] a flow system obtained by a truncation of Navier-Stokes equation,[14),22] and Rayleigh-Bénard experiment.[28] In all examples, doubling occurs only a finite number of times before the onset of chaos. This observation means the instability against a structural perturbation of the direct product state of Feigenbaum's fixed point function[33] and a torus state. In the previous letter the above conjecture was confirmed by the use of the coupled map

$$\begin{cases} X_{n+1}=1-AX_n^2+\varepsilon g(X_n,\ Y_n), \\ Y_{n+1}=Y_n+C+\varepsilon h(X_n,\ Y_n), \qquad (\mathrm{mod}\ 1) \end{cases} \tag{4·1}$$

where g and h are structural perturbations, which are periodic functions of Y with period 1. We have studied the following two cases in detail

$$\text{(I)} \qquad g(X_n,\ Y_n)=\sin(2\pi Y_n) \quad \text{and} \quad h(X_n,\ Y_n)=X_n\,, \tag{4·2}$$

$$\text{(II)} \qquad g(X_n,\ Y_n)=\sin(2\pi Y_n) \quad \text{and} \quad h(X_n,\ Y_n)=0\,, \tag{4·3}$$

where the rotation number C is fixed at an irrational number, e.g., at $(\sqrt{5}-1)/2$, i.e., the inverse of the golden mean. Model (II) can be regarded as the logistic model with an incommensurate modulation, which may be relevant as a model for the chaos with external periodic modulation or a system with a quasiperiodic modulation. If ε vanishes,

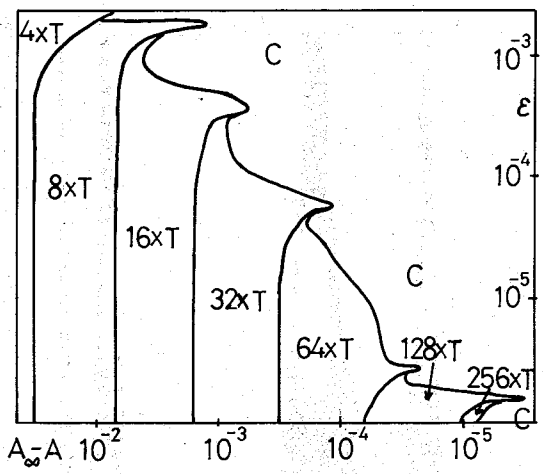

Fig. 7. Phase diagram for model (I). The transyerse axis denotes $(A_\infty - A)$, where $A_\infty (=1.401151\cdots)$ is the value of the onset of chaos for $\varepsilon=0$. The longitudinal axis denotes ε. "C" and "$n\times T$" represent chaos and $n\otimes$torus respectively.

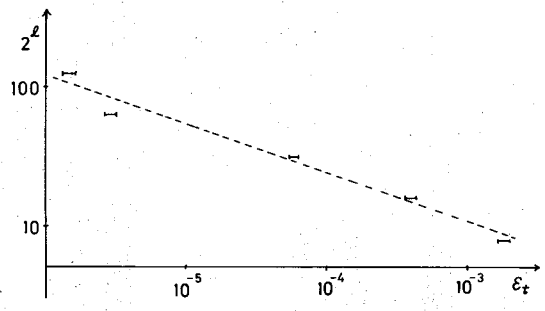

Fig. 8. Scaling relation between the strength of the coupling ε and the number of doublings l. (See text for the definition of $\varepsilon_t(l)$.)

the direct product state the "$2^k\otimes$torus" exists, which becomes unstable successively as the coupling ε is increased. (See Fig. 7.) Thus, the doubling cascade of tori occurs only a finite times in general.

As is seen from the phase diagram (Fig. 7), the number of doublings decreases as ε is increased. The scaling relation between the number of the doublings l and the strength of the coupling ε is shown in Fig. 8, where $\varepsilon_t(l)$ is the value of ε at which the "tongue" in the phase diagram (see Fig. 7) appears for the corresponding $2^l\otimes$torus-state. The scaling relation is roughly given by $2^l \propto \varepsilon_t^{-\alpha}(\alpha\sim 1/3)$, though, it seems to be impossible to obtain a quantitative result from this figure.

The above result shows that Feigenbaum's fixed point function[33] is unstable against an incommensurate modulation $\sin(2\pi(Y_0+nC))$. If the incommensurate modulation is a relevant perturbation in the renormalization group framework and the eigenvalue for this perturbation in the RG framework is given by $\varkappa$, the scaling relation

$$\alpha=\frac{\log \varepsilon_t}{\log(2^l)}=\frac{\log 2}{\log \varkappa} \tag{4·4}$$

is derived.

In the case of noisy period doublings,[34] RG theories were constructed by Crutchfield et al.[35] and Schraiman et al.,[36] which show that the relevant eigenvalue for the noisy perturbation is given by $\varkappa_{\text{noise}}=1.88995\cdots$. Thus, the scaling relation for the noisy period-doubling bifurcations is given by

$$\frac{\log \varepsilon_{\text{noise}}}{\log(2^l)}=\frac{\log 2}{\log \varkappa_{\text{noise}}}=0.366754\cdots. \tag{4·5}$$

The numerical value for the exponent on the doubling of tori ($\alpha\sim 1/3$) seems to be close to the above exponent, though it is beyond our numerical accuracy to confirm the agreement or to detect the difference between the two values.

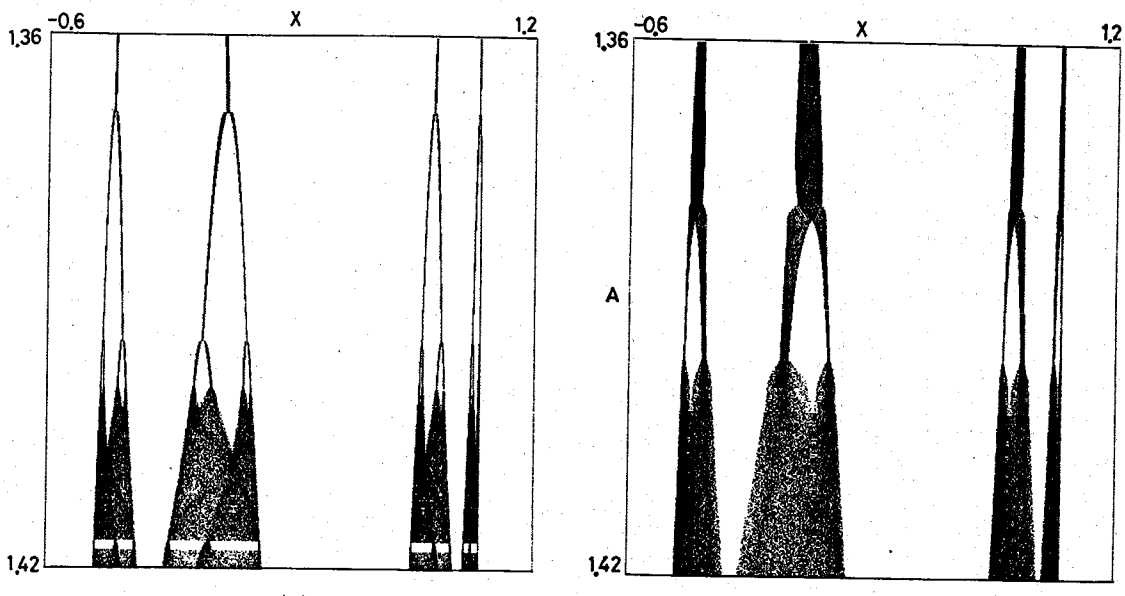

(a) (b)

Fig. 9. The orbits of x_n's $(500<n<1000)$ for model (II) with $C=(\sqrt{5}-1)/2$. The longitudinal axis denotes the bifurcation parameter A. (a) $\varepsilon=10^{-4}$ (b) $\varepsilon=10^{-3}$.

In the supercritical region, the band merging appears successively for the logistic map. For models (I) and (II), the band merging occurs only a finite number of times just as in the case of noisy period-doubling. Thus, the interruption of doubling of tori shows a "bifurcation gap", which was first observed in the noisy period-doubling bifurcation by Crutchfield and Huberman.[34] In Fig. 9, x_n's $(500<n<1000)$ are plotted as functions of the bifurcation parameter A for model (II). The bifurcation gap can be also seen from these figures.

An RG theory (if it is constructed) cannot answer the mechanism of the stop of the doubling cascade of tori by a finite number of times. At the rest of the present section we consider the mechanism of the interruption using the map (4·1) from other viewpoints than the renormalization group approach.

First, we consider the figures of the attractors when the tori are collapsed. As can be seen from Fig. 10, the oscillation of tori is enhanced at the onset of chaos. The torus seems to be fractal at the onset of chaos. Thus, the fractalization of torus[19] is a possible cause of the interruption of the doubling and the emergence of chaos.

Second, the interruption of the doubling is studied from another point of view. We consider the modulation map (II) and approximate the irrational value C by a rational value using the continued fraction expansion method.[37] Thus, the value C is replaced by $C_n=F_{n-1}/F_n$ for $C=(\sqrt{5}-1)/2$, where F_n is a Fibonacci sequence. Then F_n times iteration of the map (4·1) is reduced to the following one-dimensional mapping

$$x'=G(x)$$
$$=\varepsilon\sin(2\pi C_n(F_n-1)+f(\varepsilon\sin 2\pi(F_n-2)C_n+f(\cdots\ \cdots+f(\varepsilon\sin 2\pi C_n+f(x))\cdots) \tag{4·6}$$
$$f(x)=1-Ax^2$$

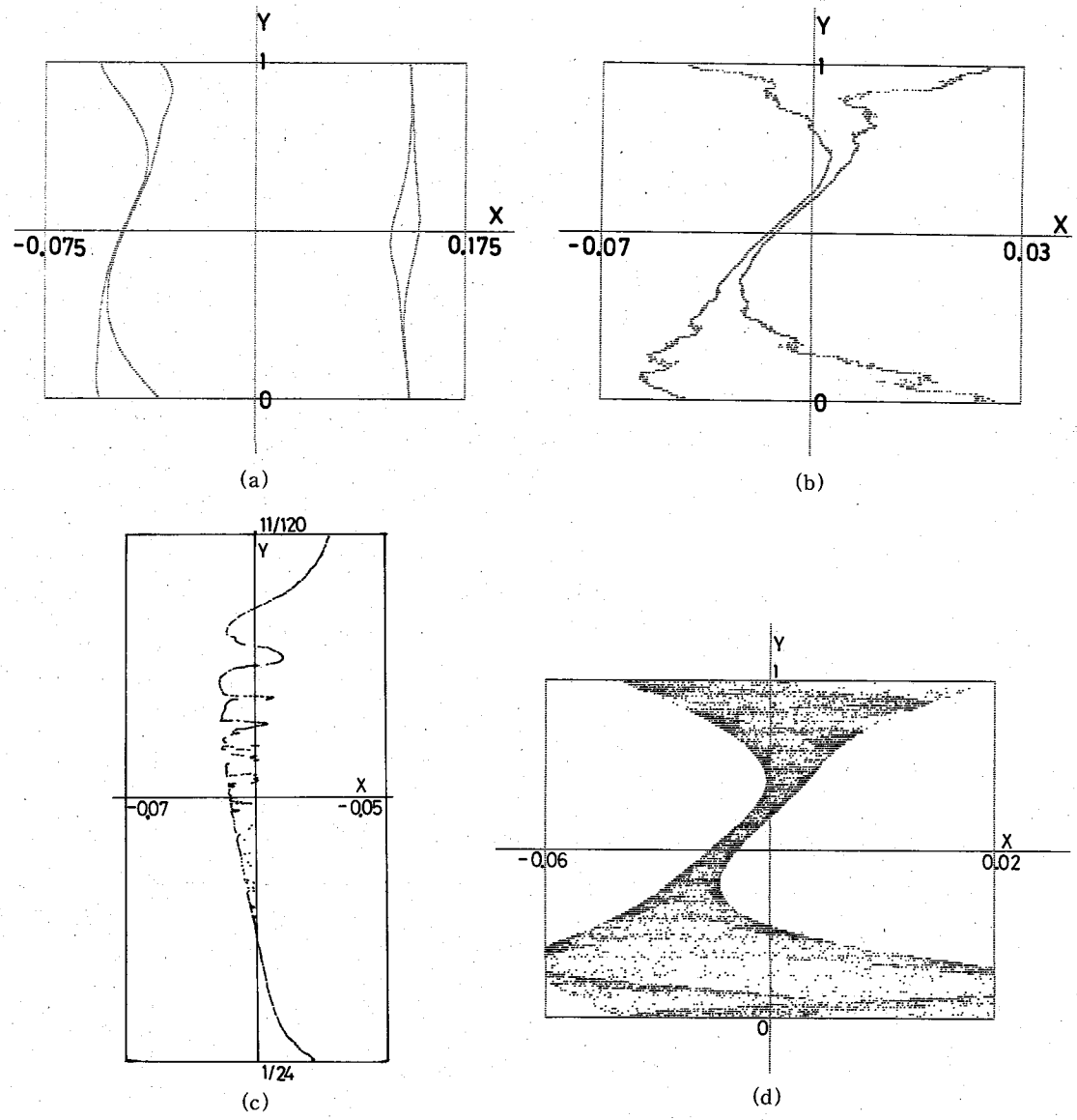

Fig. 10. Attractor of the map (4·1) (model (II)) with $C=(\sqrt{5}-1)/2$ and $\varepsilon=0.001$. (a) $A=1.3961$ (b) $A=1.3969$ (only a part) (c) $A=1.3970$ (only a part) (d) $A=1.3980$ (only a part).

for $Y_0=0$. The map (4·6) satisfies the Schwarzian condition,[38] but it is not a unimodal mapping. Thus, the period-doubling bifurcations in the map (4·6) may not continue infinitely.

As a matter of fact, we observed intermittent-like bursts between the valleys of $G(X)$, which cause the interruption of doublings and the transition to chaos [see Fig. 11) for some examples of time series by the map $G(X)$].

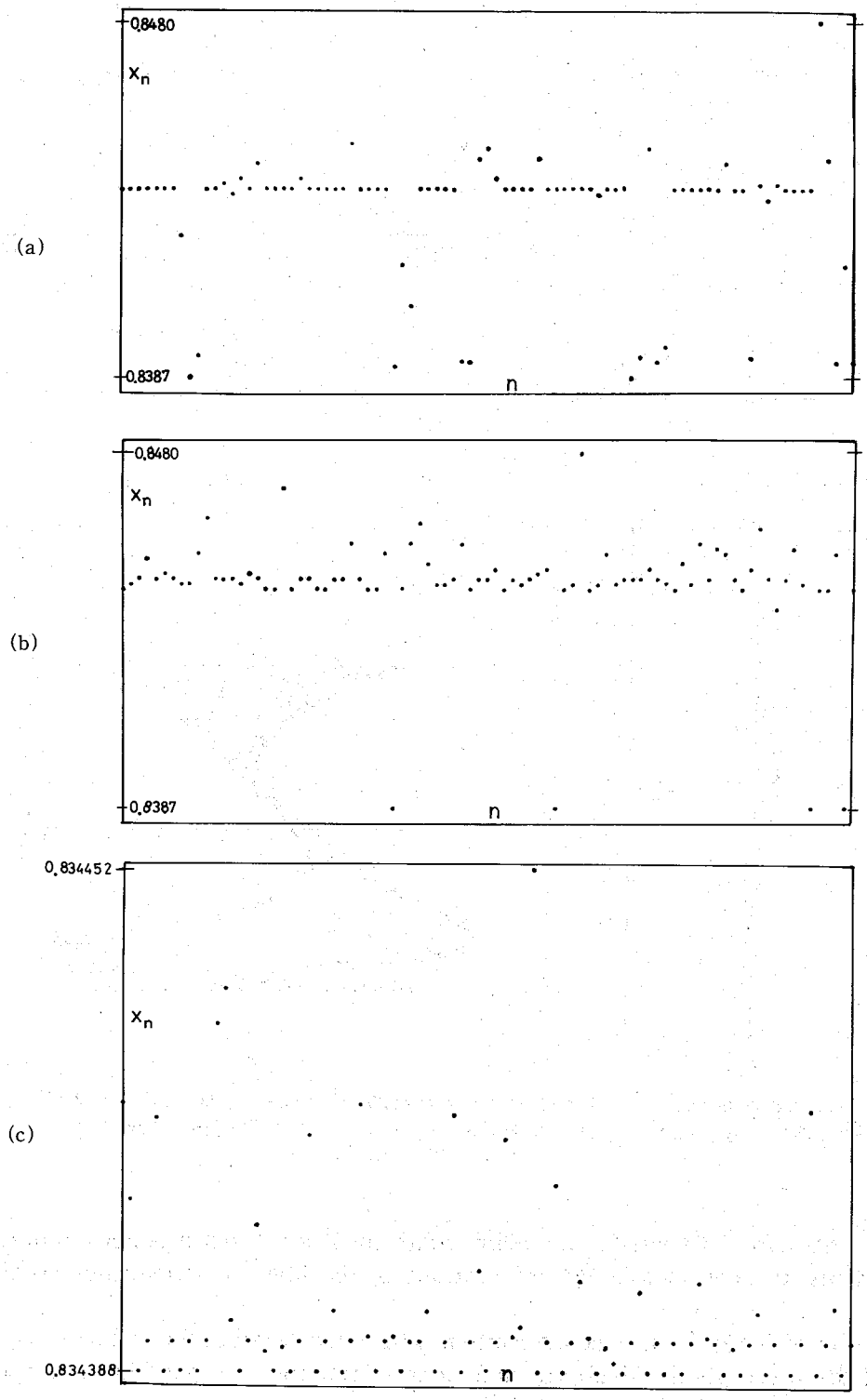

Fig. 11. Time series of the map $x_{n+1}=G^{2^k}(x_n)$ for $C=55/89$. (See text for the definition of $G(x)$.) In (a) and (b), A and ε take the values at which 32⊗torus collapses ($k=5$), while they take the values at which 64⊗torus collapses ($k=6$) in (c). (a) $A=1.4006$ and $\varepsilon=2\times10^{-4}$ (b) $A=1.40065$ and $\varepsilon=2\times10^{-4}$ (c) $A=1.401102$ and $\varepsilon=9\times10^{-6}$.

§ 5. Discussion

In the present paper, we have investigated the oscillation and doubling of tori, which are typical instabilities of amplitude motion. First, we relate the oscillation of torus to the oscillation of unstable manifolds. The oscillation can be typically seen if the stability along the amplitude direction is not strong. Oscillations of tori in the Bénard experiment will be understood from this point of view.

In usual two-dimensional mappings, however, the oscillatory behavior is masked by lockings, which appear as the instability in the phase dynamics. In order to extract only the amplitude behavior, the modulation mapping is introduced, where the fractalization of tori is discovered and analyzed.[15),19)] Fractalization of tori will be a new and typical route to chaos in the amplitude behavior of tori.

We can see the process of the development of chaos to hyperchaos using a delayed-logistic map in §2. At the onset of hyperchaos, however, we could not observe any singular behaviors. Chaos develops in the following way in our model. "Appearance of chaos through a locking"→"the dimension of the attractor grows until it becomes two (formation of the belt-like attractor)"→"width of the belt-like attractor increases"→"the unstable focus (from which the torus had appeared through Hopf bifurcation) becomes a snap-back repeller".[32)] This type of the "development of chaos" is seen in various two-dimensional mappings and may be considered to be a rather universal scenario.

In §3, we considered the oscillation of attractor from another point of view, i.e., the synergetic effect of the rotation, folding and stretching. Since the mapping which is introduced in the section is rather simple, analytic treatment will be possible for the critical phenomena of the oscillation at the onset of chaos.

When a torus is collapsed, the ordering of an orbit is lost,[11),41)] as is shown in the circle map. The disordering of an orbit is also seen in a delayed map. In the region $y>0$, the mapping $(x_n, y_n)\to(x_{n+1}, y_{n+1})$ consists of the rotation and stretching. Thus, the order of an orbit does not change in the region $y>0$. If an orbit falls in the region $y<0$, however, the folding $(y\to -y)$ occurs, which causes the disordering property of a chaotic orbit. In the delayed piecewise-linear mapping, the invariant measure in $y<0$ increases as the bifurcation parameter D is increased. Details on the disordering property in the map will be given elsewhere.

In §4, doubling of tori is reinvestigated. The mechanism of the interruption of the doubling cascade is discussed from three points of view, i.e., a relevant perturbation in an RG transformation, fractalization of tori, and the intermittent-like transition between the valleys of the multi-humped map. Quantitative study on the scaling exponent in the RG framework and on the fractal dimension on the basis of a functional mapping remains as future problems, while the relationship among the three viewpoints also has to be investigated in future.

Doublings of tori have been found in a variety of systems recently. It has been found in a simulation of the truncated Navier-Stokes equation[14)] and a system with an incommensurate modulation.[13)] Sano and Sawada have observed the doubling of tori in the Rayleigh-Bénard experiment.[28)] In these examples the doubling was observed only a few times (once or twice in usual cases) before chaos appears. The oscillatory behaviors of the torus are also seen in these examples. The map (4·1) will be an effective model to

study these phenomena.

The map (4·1) belongs to a coupled map, which is useful to study the stability of a direct product state and of a bifurcation sequence. If we replace $Y_{n+1}=Y_n+C(\mathrm{mod}\,1)$ by $Y_{n+1}=2Y_n(\mathrm{mod}\,1)$, for example, we can treat the "doubling cascade of chaos to hyper-chaos" and can show that the doubling of chaos occurs only a finite number of times. On the other hand, we can treat the torus intermittency by replacing the latter of Eqs. (4·1) by the map which gives the intermittent transition,[39] which has been extensively investigated by Daido quite recently.[16] The torus intermittency will be another important mechanism of the instability of a torus along the amplitude direction.

Acknowledgements

The author would like to thank Professor M. Suzuki for useful discussions and critical reading of the manuscript and Professor Y. Takahashi for invaluable comments. He is also grateful to LICEPP for the facilities of FACOM M190. This study was partially financed by the Scientific Research Fund of the Ministry of Education, Science and Culture.

References

1) D. Ruelle and F. Takens, Comm. Math. Phys. **20** (1971), 167.
S. Newhouse, D. Ruelle and F. Takens, Comm. Math. Phys. **64** (1978), 35.
2) S. J. Shenker, Physica **5D** (1982), 405.
M. J. Feigenbaum, L. P. Kadanoff and S. J. Shenker, Physica **5D** (1982), 370.
3) S. Ostlund, D. Rand, J. Sethna and E. D. Siggia, Physica **8D** (1983), 303.
4) K. Kaneko, Prog. Theor. Phys. **68** (1982), 669.
5) K. Kaneko, Prog. Theor. Phys. **69** (1983), 403.
6) L. Glass and R. Perez, Phys. Rev. Lett. **48** (1982), 1772.
R. Perez and L. Glass, Phys. Lett. **90A** (1982), 441.
7) L. Glass, M.R. Guerara, J. Bélair and A. Shrier, Phys. Rev. **A29** (1984), 1348.
8) M. Schell, S. Fraser and R. Kapral, Phys. Rev. **A28** (1983), 1637.
9) M. H. Jensen, P. Bak and T. Bohr, Phys. Rev. Lett. **50** (1983), 1637.
10) L. P. Kadanoff, J. Stat. Phys. **31** (1983), 1.
11) K. Kaneko, to appear in *Turbulence and Chaotic Phenomena in Fluids*, ed. T. Tatsumi (North Holland).
12) K. Kaneko, Prog. Theor. Phys. **69** (1983), 1427.
13) A. Arnéodo, P. H. Coullet and E. A. Spiegel, Phys. Lett. **94A** (1983), 1.
14) V. Franceshini, Physica **6D** (1983), 285.
15) K. Kaneko, Prog. Theor. Phys. **69** (1983), 1806.
16) H. Daido, to appear in Prog. Theor. Phys.
17) C. Grebogi, E. Ott and J. A. Yorke, Phys. Rev. Lett. **51** (1983), 339.
18) K. Kaneko, Prog. Theor. Phys. **71** (1983), 282.
19) K. Kaneko, Prog. Theor. Phys. **71** (1983), 1112.
20) J. P. Sethna and E. D. Siggia, to appear in Physica **D**.
21) H. Yahata, Prog Theor. Phys. **69** (1983), 396.
22) H. Yahata, private communication.
23) P. Bergé, Physica Scripta **T1** (1982), 71.
24) J. P. Gollub and S. V. Benson, J. Fluid Mech. **100** (1980), 449.
25) J. Maurer and A. Libchaber, J. Phys. Lett. **41** (1980), L515.
26) A. Libchaber, S. Fauve and C. Laroche, Physica **7D** (1983), 73.
27) M. Sano and Y. Sawada, to appear in *Turbulence and Chaotic Phenomena in Fluids*, ed. T. Tatsumi (North Holland).
28) M. Sano and Y. Sawada, in *Chaos and Statistical Methods*, ed. Y. Kuramoto (Springer,1984).
29) M. Sano, private communication.
30) P. Bergé, et al., J. Phys. Lett. **41** (1980), L341.
31) A review on the recent studies on the transition from torus to chaos can be seen in K. Kaneko, Ph. D. Thesis, Univ. of Tokyo, 1983 (unpublished).

32) F. R. Marotto, J. Math. Anal. Appl. **63** (1978), 199.
33) M. J. Feigenbaum, J. Stat. Phys. **19** (1978), 25; **21** (1979), 669.
34) J. P. Crutchfield and B. A. Huberman, Phys. Lett. **74A** (1980), 407.
35) J. P. Crutchfield, M. Nauenberg and J. Rudnick, Phys. Rev. Lett. **46** (1981), 933.
36) B. Schraiman, C. E. Wayne and P. C. Martin, Phys. Rev. Lett. **46** (1981), 935.
37) See e.g., J. M. Greene, J. Math. Phys. **20** (1979), 1183.
38) See e.g., P. Collet and J. P. Eckman, *Iterated Maps on the Interval as Dynamical Systems,* Birkhauser, Boston (1980).
39) Y. Pomeau and P. Manneville, Comm. Math. Phys. **74** (1980), 189.
40) K. Kaneko, to be published.
41) K. Kaneko, submitted to Prog. Theor. Phys.